

## Site Specific Relationships between COVID-19 Cases and SARS-CoV-2 Viral Load in Wastewater Treatment Plant Influent

Fitzgerald, Stephen F; Rossi, Gianluigi; Low, Alison S; McAteer, Sean P; O'Keefe, Brian; Findlay, David; Cameron, Graeme J; Pollard, Peter; Singleton, Peter T R; Ponton, George; Singer, Andrew C; Farkas, Kata; Jones, Davey L.; Graham, David W; Quintela-Baluja, Marcos; Tait-Burkard, Christine; Gally, David L; Kao, Rowland; Corbishley, Alexander

### Environmental Science and Technology

DOI:

[10.1021/acs.est.1c05029](https://doi.org/10.1021/acs.est.1c05029)

Published: 16/11/2021

Peer reviewed version

[Cyswllt i'r cyhoeddiad / Link to publication](#)

*Dyfyniad o'r fersiwn a gyhoeddwyd / Citation for published version (APA):*

Fitzgerald, S. F., Rossi, G., Low, A. S., McAteer, S. P., O'Keefe, B., Findlay, D., Cameron, G. J., Pollard, P., Singleton, P. T. R., Ponton, G., Singer, A. C., Farkas, K., Jones, D. L., Graham, D. W., Quintela-Baluja, M., Tait-Burkard, C., Gally, D. L., Kao, R., & Corbishley, A. (2021). Site Specific Relationships between COVID-19 Cases and SARS-CoV-2 Viral Load in Wastewater Treatment Plant Influent. *Environmental Science and Technology*, 55(22), 15276-15286. <https://doi.org/10.1021/acs.est.1c05029>

#### Hawliau Cyffredinol / General rights

Copyright and moral rights for the publications made accessible in the public portal are retained by the authors and/or other copyright owners and it is a condition of accessing publications that users recognise and abide by the legal requirements associated with these rights.

- Users may download and print one copy of any publication from the public portal for the purpose of private study or research.
- You may not further distribute the material or use it for any profit-making activity or commercial gain
- You may freely distribute the URL identifying the publication in the public portal ?

#### Take down policy

If you believe that this document breaches copyright please contact us providing details, and we will remove access to the work immediately and investigate your claim.

# Site specific relationships between COVID-19 cases and SARS-CoV-2 viral load in wastewater treatment plant influent

Stephen F. Fitzgerald<sup>\*1</sup>, Gianluigi Rossi<sup>\*1</sup>, Alison S. Low<sup>1</sup>, Sean P. McAteer<sup>1</sup>, Brian O’Keefe<sup>2</sup>, David Findlay<sup>2</sup>, Graeme J. Cameron<sup>2</sup>, Peter Pollard<sup>2</sup>, Peter T. R. Singleton<sup>2</sup>, George Ponton<sup>3</sup>, Andrew C. Singer<sup>4</sup>, Kata Farkas<sup>5,6</sup>, Davey Jones<sup>5</sup>, David W Graham<sup>7</sup>, Marcos Quintela-Baluja<sup>7</sup>, Christine Tait-Burkard<sup>1</sup>, David L. Gally<sup>1</sup>, Rowland Kao<sup>#1</sup>, Alexander Corbishley<sup>#1</sup>

<sup>\*</sup>Authors contributed equally

<sup>#</sup> Joint communicating authors [alexander.corbishley@roslin.ed.ac.uk](mailto:alexander.corbishley@roslin.ed.ac.uk) [rowland.kao@ed.ac.uk](mailto:rowland.kao@ed.ac.uk)

<sup>1</sup> The Roslin Institute and Royal (Dick) School of Veterinary Studies, The University of Edinburgh, Easter Bush Campus, Midlothian, EH25 9RG, UK

<sup>2</sup> Scottish Environment Protection Agency, Strathallan House, Stirling, FK9 4TZ, UK

<sup>3</sup> Scottish Water, Castle House, 6 Castle Drive, Dunfermline, KY11 8GG

<sup>4</sup> UK Centre for Ecology & Hydrology, Wallingford, OX10 8BB, UK

<sup>5</sup> School of Natural Sciences, Bangor University, Deiniol Road, Bangor, Gwynedd, LL57 2UW, UK

<sup>6</sup> School of Ocean Sciences, Bangor University, Menai Bridge, Anglesey, LL59 5AB, UK

<sup>7</sup> School of Engineering, Newcastle University, Newcastle upon Tyne NE1 7RU, UK

**Keywords:** epidemiology, sewage, influent, coronavirus, RNA

## Synopsis

There is a strong, site specific, relationship between COVID-19 cases and SARS-CoV-2 viral RNA load in wastewater treatment plant influent.

## Abstract

Wastewater based epidemiology (WBE) has become an important tool during the COVID-19 pandemic, however the relationship between SARS-CoV-2 RNA in wastewater treatment plant influent (WWTP) and cases in the community is not well defined. We report here the development of a national WBE program across 28 WWTPs serving 50% of the population of Scotland, including large conurbations, as well as low-density rural and remote island communities. For each WWTP catchment area, we quantified spatial and temporal relationships between SARS-CoV-2 RNA in wastewater and COVID-19 cases. Daily WWTP SARS-CoV-2 influent viral RNA load, calculated using daily influent flow rates, had the strongest correlation ( $p > 0.9$ ) with COVID-19 cases within a catchment. As the incidence of COVID-19 cases within a community increased, a linear relationship emerged between cases and influent viral RNA load. There were significant differences between WWTPs in their capacity to predict case numbers based on influent viral RNA load, with the limit of detection ranging from twenty-five cases for larger plants to a single case in smaller plants. SARS-CoV-2 viral RNA load can be used to predict the number of cases detected in the WWTP catchment area, with a clear statistically significant relationship observed above site-specific case thresholds.

## Introduction

The COVID-19 pandemic has necessitated the rapid implementation of surveillance programs worldwide to track and control the spread of SARS-CoV-2 (the coronavirus that causes the disease syndrome known as COVID-19). Initially, such programs relied on syndromic surveillance, community testing, contact tracing and the monitoring of morbidity and mortality rates <sup>1-3</sup>. Community testing relies on voluntary reporting of clinical signs and is only partially able to capture the pre-symptomatic, asymptomatic and pauci-symptomatic cases of SARS-CoV-2 infection that can contribute significantly to community transmission, and are therefore subject to biases, which can influence estimates of disease burden <sup>1, 2</sup>. Syndromic surveillance based on hospital admissions is less biased, but is subject to delays between infection and admission <sup>2</sup>, while implementing mass swab-testing on a nationally meaningful scale is not economically feasible for most countries <sup>2</sup>. Early studies identified SARS-CoV-2 RNA in the feces of infected individuals and COVID-19 has subsequently been associated with a range of gastrointestinal symptoms <sup>4</sup>. SARS-CoV-2 has been detected in feces from both asymptomatic and symptomatic individuals, with prolonged shedding observed up to 33 days after the initial onset of symptoms or hospitalization <sup>1, 4, 5</sup>. Consequentially, wastewater-based epidemiology (WBE) has been explored as a tool to track the spread of SARS-CoV-2 by many countries <sup>1</sup>. Early in the pandemic, Medema *et al.*<sup>6</sup> detected SARS-CoV-2 RNA in the wastewater of three Dutch cities and a major airport up to six days before the first reported clinical cases <sup>6</sup>. Since then, WBE programs have been started by over 50 countries <sup>1, 7, 8</sup>, however a number of important questions remain relating to the implementation of these programs and the interpretation of WBE data. These include the impact of viral shedding dynamics in feces, viral persistence in wastewater and wastewater flow rates on viral detection in wastewater,

whether differences exist between urban and rural wastewater systems and how viral levels in wastewater should be normalized with respect to population size <sup>2</sup>. Furthermore, there are a range of techniques available for detecting viruses in wastewater, whilst wastewater samples are diverse with respect to their physicochemical composition. There is therefore a need to determine which methodologies and process controls are appropriate when operationalizing WBE at a national scale <sup>2</sup>.

This study describes the development and implementation of a national WBE SARS-CoV-2 surveillance program. We compared and optimized commonly used viral concentration techniques, validated Porcine Respiratory and Reproductive virus (PRRSv) as a suitable process control and optimized RT-qPCR assays for SARS-CoV-2 detection in wastewater. This methodology was adopted by the Scottish Environment Protection Agency (SEPA) and has been used to routinely monitor viral levels at 28 wastewater treatment plant (WWTP) sites across Scotland, serving 50% of the Scottish population (2.66 million people). These sites include large conurbations, as well as low-density rural and remote island communities. We demonstrate that daily SARS-CoV-2 viral RNA load can be used to predict the number of cases detected in the WWTP catchment area, with a clear statistically significant relationship observed between these two variables above site-specific case thresholds.

## **Methods**

### **WWTP site selection**

WWTP monitoring sites were selected by Scottish Water and SEPA to represent at least 50% of the population in each Scottish health board area (Table S2.1), using the minimum number of sites possible.

### **Wastewater sample collection**

WWTP influent was collected at most sites using a refrigerated autosampler that obtained a fixed volume of influent every hour over each 24-hour period (08:00 to 08:00). Refrigerated autosamplers at Dalbeattie, Allanfearn, Nigg and Fort William obtained a fixed volume of influent, where the frequency of sampling over each 24-hour period was dependent on the influent flow rate. Composite 24-hour samples were mixed prior to analysis. Sites were typically sampled once a week, with increased frequency of sampling in response to increases in disease incidence in the community. There was no specific disease incidence threshold that was used to determine sampling frequency, however the local directors of public health were consulted, with sampling prioritized according to local needs. Due to resource limitations, any single site was not sampled more than four times a week. Samples were transported and stored at 4°C prior to analysis, typically within 24-48 hours of collection.

#### **Wastewater concentration and detection of SARS-CoV-2**

Five viral concentration methods, Methods 1 – 5, based on filtration, precipitation and adsorption were trialed (see Supporting Information). Method 1 was further optimized by SEPA (Method 6) and used for routine wastewater monitoring. Viral RNA was extracted from concentrated wastewater samples using commercial kits (see Supporting Information). SARS-CoV2 was detected by RT-qPCR. During method development (April-May 2020), there was a national shortage of RT-qPCR reagents, with a number of suppliers providing contaminated oligonucleotides. Early experiments consequently relied on E gene detection, however once uncontaminated N1 gene reagents were available, performance of the E gene and N1 gene assays was compared using RNA extracted using multiple methods. Detection of the N1 gene was used during routine monitoring.

#### **Data collection**

Two WWTP datasets were provided by SEPA via a publicly available portal<sup>9</sup>. The first dataset reported sample date, location (WWTP name, coordinates, Health Board, and Local Authority), catchment area (CA) size (population band and population) and SARS-CoV-2 N1 and E gene average concentrations (gene copies/l). The second dataset reported the daily WWTP influent flow (l/day) and three separate N1 gene technical replicates for each sample. All replicates (838 of 2967) not returning a detectable signal were marked as “negative” in the dataset, and they were treated as zeros in the analyses. SEPA also provided the WWTP dry weather (i.e. licensed) flow (l/day) and Scottish Water provided the CA shapefiles for the 28 sites.

COVID-19 data in Scotland are collected by Public Health Scotland (PHS) and the dataset used in this study reports the date and location of first COVID-19 tests and first positive tests (i.e. such that ‘positivity’ is the proportion of individuals who test positive), with test results, and deaths, starting from March 1<sup>st</sup>, 2020. To protect patient anonymity, data were provided by PHS by “datazone”, a small-scale geographic unit identified by the National Records of Scotland (NRS) containing approximately 500 to 1000 individuals. Each case was assigned to a datazone on the basis of the patients’ reported address of residence, irrespective of where any treatment or testing was administered. Datazone size was set to avoid the need to mask any data to protect patient confidentiality i.e. each datazone is large enough so that the identity of a case cannot be inferred from other publicly available information. Relevant shapefiles and population data were downloaded from the NRS portal<sup>10</sup>, facilitating a high resolution allocation of the number of tests, detected cases (i.e. positive tests), and COVID-19 related deaths for each of the CAs.

## **Data analysis**

The objective was to understand the association between the concentration and daily viral RNA load of SARS-CoV-2 RNA in WWTP influent and the number of detected cases in the corresponding CA. The daily WWTP influent viral RNA load was calculated by multiplying the wastewater sample viral RNA concentration with the total WWTP influent flow for the day of sampling. Since daily flow is not always available, SEPA included a flow estimate obtained with a linear regression model that considered ammonium concentration (provided by Scottish Water), catchment population, and site as independent variables (Roberts and Fang, private communication). Analyses were repeated using both reported flow rates and these estimates (see Supporting Information).

The number of detected cases and the positive test rate were calculated by counting the number of positive and total tests over the seven days up to and including the day the sample was taken. We undertook a sensitivity analysis to test the effect of varying this time period from zero days i.e. counting only the reported cases on the day of wastewater sample collection) to 28 days on our results (see Supporting Information).

First, a simple correlation between viral concentration or load and number of cases or positive test rate was calculated using Spearman's  $\rho$  rank correlation coefficient.

Further, to test the association between observed cases ( $Y_{i,j}$ ) and daily WWTP viral RNA load ( $X_{i,j}$ ), we fitted a basic linear mixed model <sup>11</sup>

$$Y_{i,j} = \beta_0 + \beta_1 X_{i,j} + u_j + b_j X_{i,j} + \varepsilon_i ,$$

where  $\beta_0$  and  $\beta_1$  represent the fixed intercept and coefficient of the daily WWTP viral RNA load  $X_{i,j}$ . Parameters  $u_j$  and  $b_j$  are the random intercept and coefficient, associated with each group  $j$  (catchment), while  $\varepsilon_i$  represents the error term. We used this model to allow both the intercept and the slope (i.e. the coefficient of the daily viral load) to be composed by a common and a group-specific part, therefore for each site  $j$  the final intercept and slope



were, respectively,  $\beta_0 + u_j$  and  $\beta_1 + b_j$ . The addition of a random slope was verified with a Chi<sup>2</sup> test <sup>12</sup>. Before the estimation, the dependent and independent variables were square root transformed, which was required to reduce the overdispersion of the distribution prior to linear mixed model analysis (the untransformed data are reported in Fig S2.9, which shows the daily viral load average of the three sample replicates).

We evaluated the model using the conditional pseudo-R<sup>2</sup>, which measures the variance explained by both fixed and random effects <sup>12</sup> and analyzed the resulting coefficients (intercept,  $\beta_0 + u_j$ , and slope,  $\beta_1 + b_j$ ) to assess the consistency of the signal and the potential causes of the differences between WWTPs. We first fitted a series of univariable linear regression models with the site's slope or intercept as the dependent variable and population, population density, number of wastewater samples, latitude, longitude, deprivation and access indices <sup>10</sup> as independent variables. Deprivation and access indices measure the relative deprivation and the access to healthcare services respectively of a datazone. They were included as potential causes of bias in case detection. We then fitted a multivariable model to each coefficient, selecting as independent variables those returning a *p*-value below 0.2 in the univariable models. This threshold was chosen to allow the inclusion of variables not significant when considered in isolation, but potentially significant in a multivariable model. Variables were then further selected through a backward stepwise selection in order to eliminate the statistically insignificant ones, using the Akaike Information Criterion (AIC) for evaluation.

All data analyses were done in R 4.0.1 <sup>13</sup>, using packages *tidyverse* 1.3.1 <sup>14</sup>, *scales* 1.1.1 <sup>15</sup> and *ggrepel* 0.9.1 <sup>16</sup> for data manipulation and representation, and packages *lme4* 1.1.27.1 <sup>17</sup>, and *MuMIn* 1.43.17 <sup>18</sup> for the mixed model fit and evaluation.

## Results

### Method optimization and detection of SARS-CoV-2 RNA in WWTP influent

Reliable quantification of SARS-CoV-2 in wastewater requires consistent viral RNA extraction across a broad range of concentrations. To investigate this, aliquots of a single wastewater sample were spiked with a serial dilution of heat-inactivated SARS-CoV-2. There was no association between viral concentration and the efficiency of RNA recovery across five orders of magnitude of SARS-CoV-2 concentration (Fig S1.1.A). Significantly more SARS-CoV-2 ( $p > 0.0001$ ) was recovered at a  $10^{-2}$  dilution, however there was no evidence that this anomaly was due to PCR inhibition, as no further increase in recovery was observed upon further sample dilution. As recovery across all other dilutions was comparable, we suggest this higher efficiency of recovery at  $10^{-2}$  was the result of handling error. We next validated PRRSv (a porcine enveloped nidovirus that can be cultured *in vitro* at Containment Level 2) as a suitable surrogate process control virus for SARS-CoV-2. The extraction efficiency of heat-inactivated SARS-CoV-2 was statistically significantly greater than either live PRRSv ( $p = 0.0348$ ) or heat-inactivated PRRSv ( $p = 0.0056$ ) (Fig S1.1.B) when spiked into a single wastewater sample, however it was within the same order of magnitude (approx. 1% vs. 2%). Extraction efficiencies were also comparable between SARS-CoV-2 and heat-inactivated PRRSv within wastewater samples from six individual WWTPs ( $p > 0.05$ ) (Fig S1.1.C). Heat-inactivated PRRSv was chosen as a process control for all subsequent testing.

Viral concentration methodologies based on filtration (Methods 1 - 3), PEG precipitation (Method 4) and adsorption (Method 5) were compared. The requirement to stir larger sample volumes for 8 h made the milk powder adsorption method insufficiently scalable and so it was excluded following initial pilot trials. PRRSv was recovered more efficiently by filtration than PEG precipitation from samples WWTP2 ( $p = 0.0162$ ) and WWTP5 ( $p =$

0.0382) and heat-inactivated SARS-CoV-2 was also recovered more efficiently by filtration from sample WWTP2 ( $p < 0.0001$ ) but not WWTP5 ( $p = 0.3623$ ) (Fig S1.1.D). There was no difference in the recovery of PRRSv when spiked with heat-inactivated SARS-CoV-2 from either WW sample. More variability between technical replicates was also observed using PEG precipitation (Fig S1.1.D).

We compared liquid phase (influent and effluent) and solid phase (primary sludge and dewatered cake) samples for use in detection of SARS-CoV-2 RNA. Samples were taken weekly from a single plant, WWTP2, over a three-week period. The median recovery of PRRSv from influent was 20% across the 3-week sample period (Fig S1.1.E), however SARS-CoV-2 RNA levels were below the limit of quantification (Fig S1.1.F).

SARS-CoV-2 RNA was detected in all primary sludge samples and 2/3 dewatered cake samples from WWTP2 despite poor recovery of PRRSv from both sludge (0.5 – 3.5%) and dewatered cake (0.2 – 0.8%). No SARS-CoV-2 RNA was detected in the effluent from WWTP2 (n=3 technical replicates taken weekly over 3 consecutive weeks), however it should be noted that influent loading of SARS-CoV-2 RNA at WWTP2 during this time was close to the limit of detection and so the presence of SARS-CoV-2 in effluent at higher influent loads cannot be excluded. Although sludge and/or dewatered cake may be a more sensitive sample type for detection of SARS-CoV-2<sup>19</sup>, due to sampling difficulty and differences in sludge processing methods among WWTPs, influent samples were chosen for subsequent testing. Furthermore, some WWTPs treat sludge from other sites and hence sludge may not always be representative of the WWTP CA.

As Method 1 was both scalable and was less variable for viral recovery efficiency than PEG precipitation, this method was selected to determine if SARS-CoV-2 RNA could be detected and quantified in wastewater collected from WWTPs in Scotland during the start of the

pandemic. Influent samples from six wastewater treatment plants, WWTP1 – WWTP6, were tested (Fig S1.2). Samples were taken on 27<sup>th</sup> March 2020, shortly before the first COVID-19 mortality peak in Scotland. A strong positive SARS-CoV-2 RNA signal of 18,000 genome equivalents per liter was detected in sample WWTP5 (Fig S1.2.A). SARS-CoV-2 RNA levels in each of the other five plants fell below our limit of quantification. Method 1 was further optimized by SEPA (Method 6; Supporting Information) and used for routine wastewater monitoring. Of note, detection of the N1-gene by RT-qPCR was found to be more sensitive than the E-gene (Fig S1.2.B) and therefore N1-gene detection was adopted for the national program.

#### **Data analysis**

The weekly number of SARS-CoV-2 reported cases, deaths and positivity are shown in Fig 1A. As of 29/1/2021, 989 wastewater samples, with three technical replicates each, have been analyzed across 28 WWTPs, with the earliest samples taken from late May 2020 (Fig 1B). The number of samples per WWTP ranged from 12 (Stornoway, Outer Hebrides) to 112 (Shieldhall, Greater Glasgow). The CAs are distributed across Scotland (Fig 1C) and despite covering only 1.2% of Scotland's land mass, they cover 50% of the population. Daily WWTP influent flow data was missing for 18% of the samples.

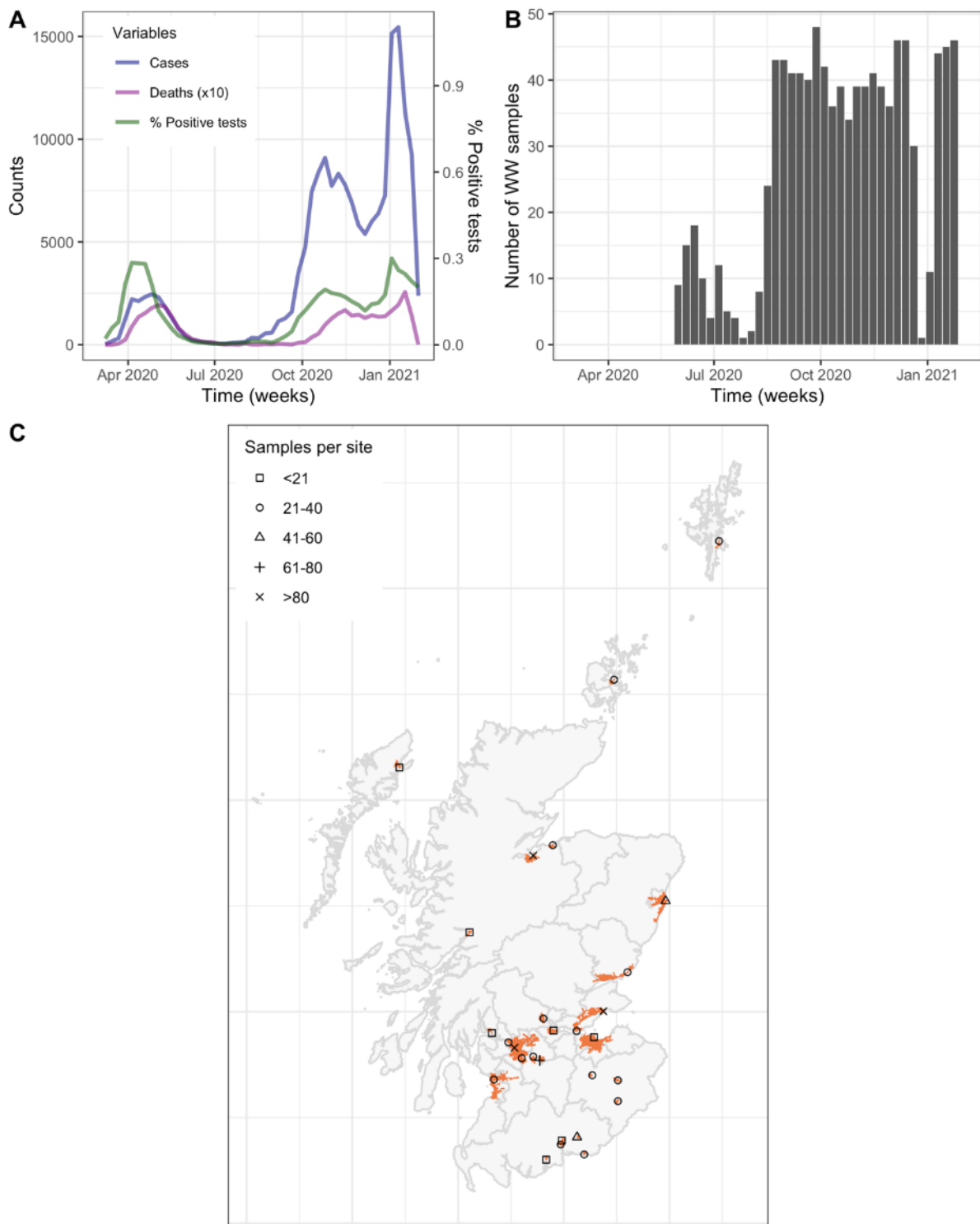


**Figure 1.** A, Number of weekly COVID-19 cases, deaths (multiplied by ten, for visualization purposes), and positive test rate in Scotland; B, weekly number of wastewater samples across the 28 study sites; C, spatial distribution of the 28 wastewater treatment plant sites with their catchment area (orange). Shape denotes the total number of samples by site (square: less than 20, circle: 21 to 40, triangle: 41 to 60, plus: 61 to 80, cross: over 80).

261 As evident in Fig 2, wastewater RNA viral concentration (panels A, C and E) and daily WWTP  
262 viral RNA load (panels B, D, and F) mimic the trends of the daily positive test rate (number of  
263 positive tests over the total) and the daily incidence curves, respectively. This was  
264 independent of the CA population size (Fig S2.1 to S2.5 for remaining WWTPs).  
265

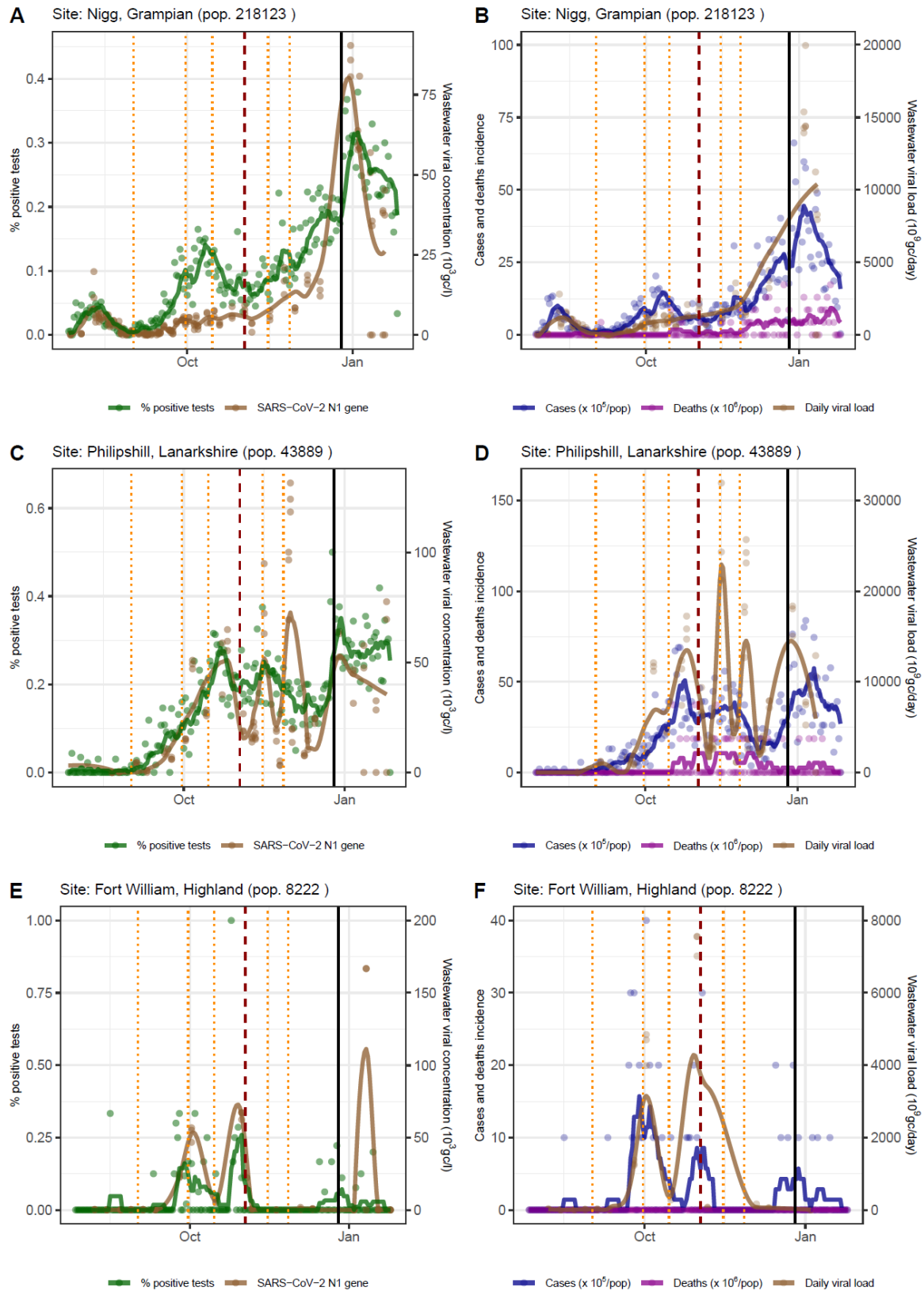


**Figure 2.** Trends of the first test positivity rate (green) and SARS-CoV-2 N1 gene concentration (brown, gc/l) in wastewater samples (panels A, C, and E); trends of COVID-19 incidence per 100,000 people (blue), deaths per 1,000,000 people (purple), and N1 gene daily load (brown, gc/day) in wastewater samples (panels B, D, and F).

For positive test rate, cases, and deaths, points represent the daily value, and lines the seven-day rolling mean. For N1 gene concentration and daily load, points represent each reading of the samples, and the line was obtained by fitting a locally estimated scatterplot smoothing (LOESS) function. Data for three sites of different size are visualized here: Nigg (Grampian, panel A and B), Philipshill (Lanarkshire, panel C and D), and Fort William (Highland, panel E and F). The remaining 25 are shown in the Supporting Information. Vertical lines mark the changes in restrictions: local or minor policy changes (orange dotted lines), the introduction of the regional tier system (dashed red line) and the post-Christmas national lockdown (black thick line). LOESS fitting was undertaken using the fANCOVA R package (v0.6-1)<sup>20</sup>, which allows automatic selection of the smoothing parameter.

Preliminary correlation analyses between the WWTP daily viral RNA concentration and the number of COVID-19 cases detected in the CA in the previous week resulted in a Spearman's  $\rho = 0.79$ , while the correlation between WWTP viral concentration and positive test rate resulted in  $\rho = 0.83$ . Using the viral load (i.e. multiplying the concentration by the WWTP daily flow rate), the correlation improved for the number of cases,  $\rho = 0.91$ , while it decreased for the positive test rate,  $\rho = 0.77$  (all  $p \sim 0$ ). This result was robust to the choice of the period length considered to calculate the number of cases or the positive test rate (see Fig S2.6). In this case, the correlations improve as the number of contributing days for case counts before sampling increases from zero to five, at which point it stabilizes.

The full mixed model explained 78% of the variance in the number of cases in the CA (conditional  $R^2 = 0.78$ ), while the daily viral RNA load as a fixed effect (i.e. the component of the slope constant across all sites) explained 45% of the variance (marginal  $R^2 = 0.45$ ). The null hypothesis that the sites' random slope variance was zero, which can be interpreted as the absence of significant differences between the cases-viral load relationship strength



295 across sites, was rejected with a  $\chi^2$  test ( $p \sim 0$ ). The normality assumption about the  
296 distribution of model residuals was verified graphically (Fig S2.10). When the model was re-  
297 run using a different time period to calculate the number of detected cases, the conditional  
298  $R^2$  ranged from 0.71 to 0.89, with an average of 0.76 across the 29 periods considered (Fig  
299 S2.11).

300 The mixed model fit by site is reported in Fig 3 (and Fig S2.12). While the daily WWTP viral  
301 RNA load coefficients, or slope, are an indicator of the strength of the relationship between  
302 viral RNA load and cases, the intercept provides an estimate of the limit of detected cases in  
303 each CA.

304

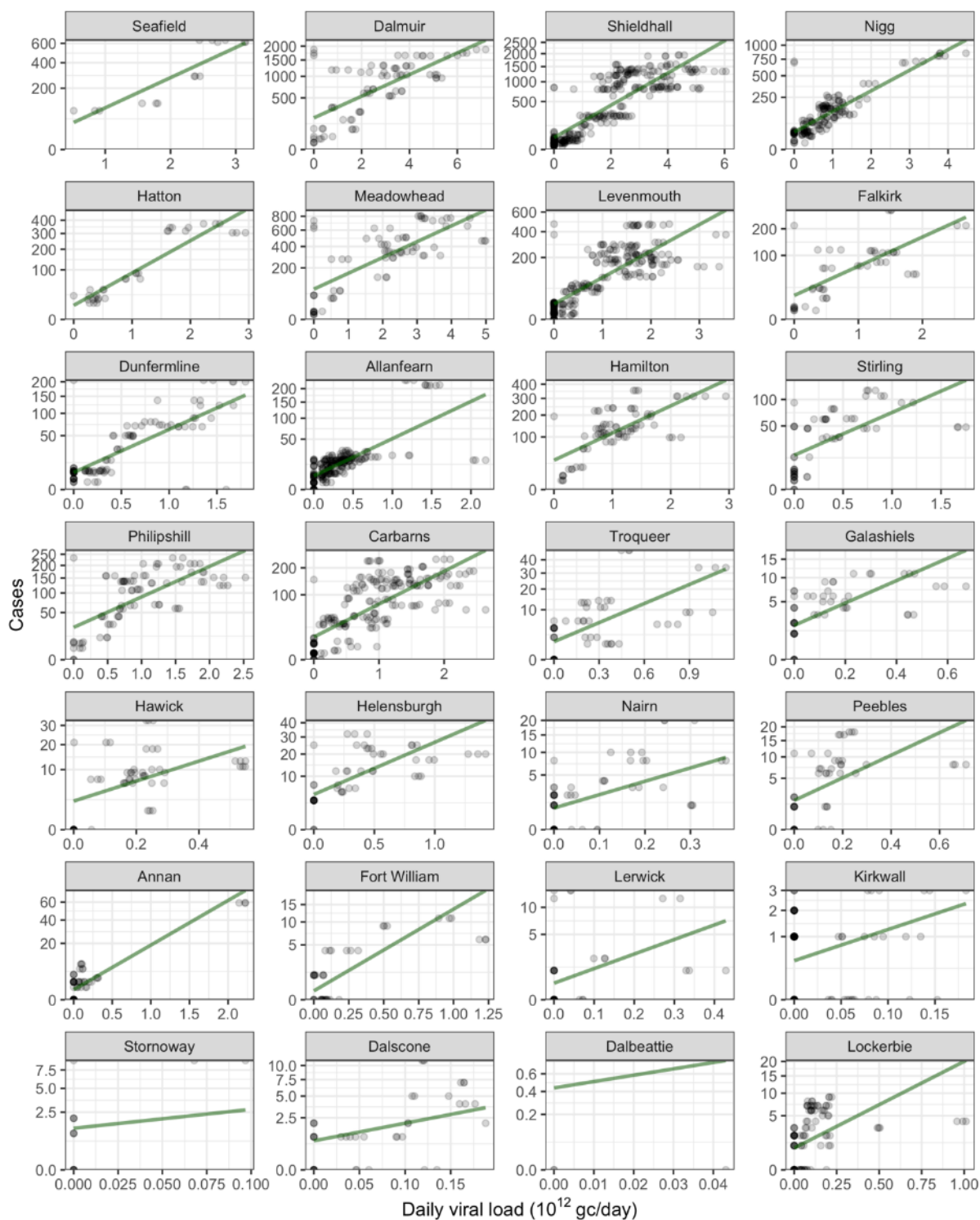


**Figure 3.** Linear regression mixed model fit for the 28 wastewater treatment plants, ordered by their catchment population size. Each WWTP regression is plotted with independent axes limits, see Figure S.2.10. for a version of the plot with fixed axes. Grey dots represent the observations, the green lines represent the regression model fit.

The median [interquartile] estimated slope across sites was  $5.2 \times 10^6$  [ $4.50$ - $5.37 \times 10^6$ ], and was positive in all sites, including the confidence interval (Fig 4A). The median [interquartile] intercept was 2.01 [0.90-3.77]. The intercept varied substantially between WWTPs of different size: median 0.84 [0.63-0.90] for the smaller sites (< 10,000 population), 2.25 [1.72-3.78] for the medium-sized sites (10,000 to 100,000 population), and 5.30 [3.2-6.95] for the larger sites (> 100,000 population). This translates to a threshold of less than one recorded case from which the relationship between viral RNA load and cases is detectable in small catchments, five recorded cases in the medium-sized catchments and twenty-five cases in the large catchments. Among the latter group, Dalmuir and Meadowhead were outliers, with higher intercept and lower slope compared with similar-sized catchments (Fig 4C).

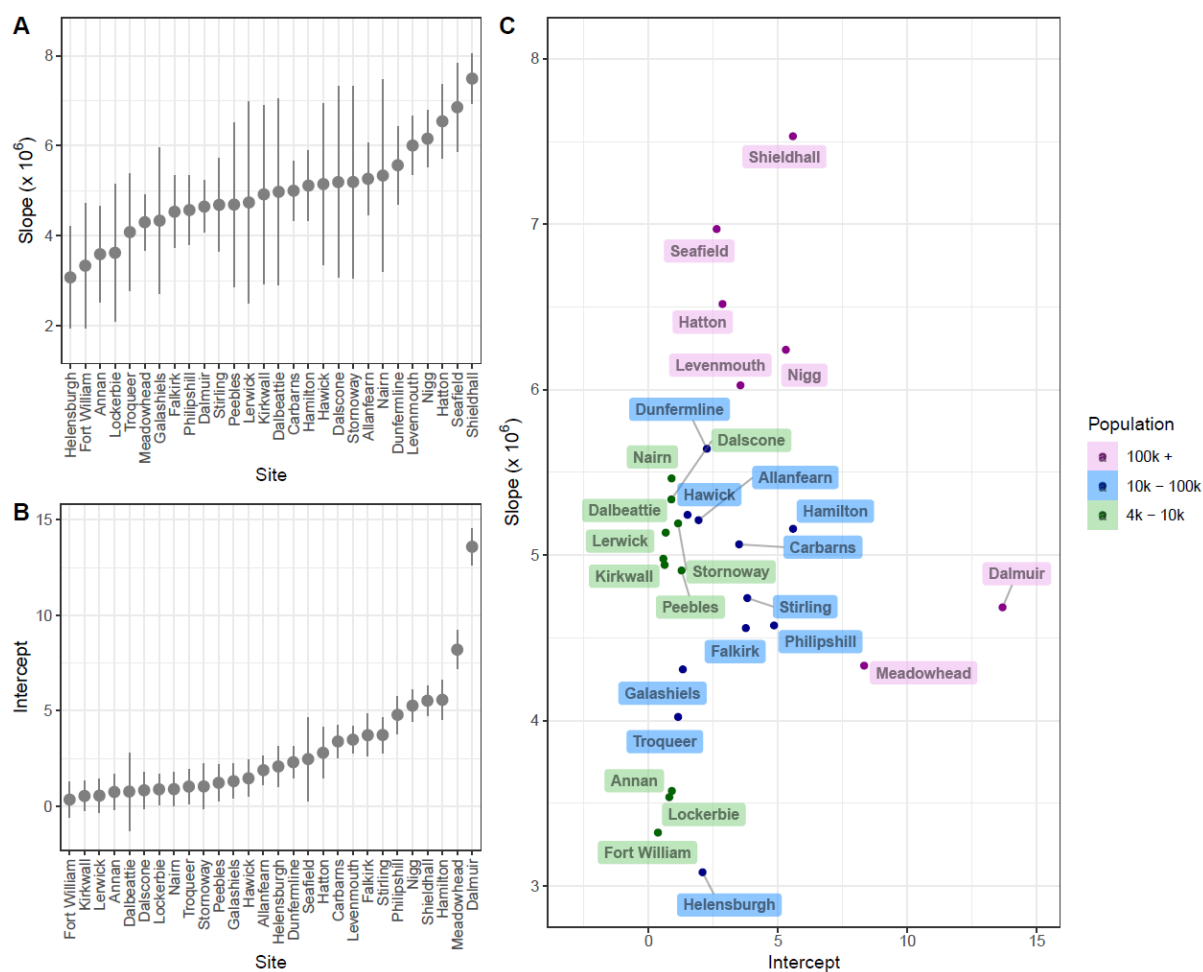


**Figure 4.** Linear mixed model coefficients: slopes (panel A) and intercept (panel B), ordered by coefficient size.

Points correspond to the mean and bars correspond to confidence interval. Panel C shows the relationship between slope and intercept, with points and labels colored by catchment population size.

The variables that best explain differences in mixed model slopes across WWTPs were the population size and the number of samples taken, although geographical longitude (not significant) was retained after multivariable model stepwise selection (Table 1). The CA population size and deprivation index were significant in explaining the differences in the mixed model intercepts (see Fig S2.10 for single variable plots).

Dependent variable	Independent variable	Univariable linear model		Multivariable linear model	
		Coefficient	<i>p</i>	Coefficient	<i>p</i>
<b>Mixed model groups slopes</b>	<i>Number of samples</i>	<b>0.42</b>	<b>0.012</b>	<b>0.30</b>	<b>0.042</b>
	<b><i>Population</i></b>	<b>0.56</b>	<b>&lt;0.001</b>	<b>0.47</b>	<b>0.003</b>
	<i>Density</i>	0.27	0.129	(dropped by stepwise selection)	
	Latitude	0.15	0.435	-	-
	<i>Longitude</i>	<b>0.31</b>	<b>0.179</b>	0.28	0.109
	Deprivation index	0.15	0.373	-	-
	<i>Access index</i>	<b>-0.44</b>	<b>0.007</b>	(dropped by stepwise selection)	
	<i>Multivar. intercept</i>	-	-	0.15	0.133
<b>Mixed model groups intercepts</b>	Number of Samples	0.20	0.236	-	-
	<b><i>Population</i></b>	<b>0.53</b>	<b>&lt;0.001</b>	<b>0.45</b>	<b>0.002</b>
	<i>Density</i>	<b>0.48</b>	<b>0.001</b>	(dropped by stepwise selection)	
	Latitude	-0.16	0.370	-	-
	Longitude	-0.25	0.242	-	-
	<b><i>Deprivation index</i></b>	<b>0.37</b>	<b>0.009</b>	<b>0.27</b>	<b>0.030</b>
	<i>Access index</i>	<b>-0.42</b>	<b>0.005</b>	(dropped by stepwise selection)	
	<i>Multivar. intercept</i>	-	-	0.01	0.908

335

336 **Table 1.** Results of the univariable and multivariable linear models to determine the variables that influence  
337 the mixed model slope and intercept for different sites. The R<sup>2</sup> of the two multivariable linear models was 0.45  
338 for the slope, and 0.50 for the intercept (both  $p < 0.001$ ).

339

## Discussion

SARS-CoV-2 WBE has rapidly become an important surveillance tool for COVID-19 around the world, with studies from a number of countries identifying a close relationship between SARS-CoV-2 levels in wastewater and COVID-19 cases in the CA, including in the USA<sup>21-24</sup>, Australia<sup>25</sup>, France<sup>26</sup>, and Spain<sup>27</sup>. Importantly, our work uniquely describes the establishment of a WBE program covering 50% of a country's population across a wide range of WWTP sizes. We demonstrate how WBE can be adopted across a range of catchments, from densely populated urban areas (Edinburgh and Glasgow), to smaller towns, rural areas and islands.

We have used granular geospatial data to determine accurate estimates of recorded COVID-19 cases within each CA and demonstrate the existence of a strong and measurable statistically significant relationship between the SARS-CoV-2 daily WWTP viral RNA load and the number of detected cases in the week preceding wastewater sample collection. Whilst the importance of using viral load, rather than viral concentration, has been demonstrated by other authors<sup>24</sup>, we have gone further to validate the use of ammonium concentration to calculate viral load when daily influent flow data is missing. We have also used granular geospatial and longitudinal data to characterize, in detail, the relationship between viral load and community cases over the month preceding sample collection.

In keeping with work examining levels of SARS-CoV-2 RNA in WWTP settled solids<sup>22</sup>, we show that the precision of the relationship between influent viral load and community cases varies between sites, with differences in the slope mostly attributed to the size of the population being served. Our results identified a stronger relationship between cases and viral RNA load in the larger WWTPs. Uniquely, we also explored the impact of population density, longitude, latitude, and deprivation and healthcare access indexes on the

relationship between influent viral load and community cases. The identified threshold for detection was typically under 25 cases, and for some smaller WWTPs, a single detected community case was sufficient to yield a positive wastewater result. Compared to similar-sized WWTPs, Meadowhead and Dalmuir were outliers (Fig 4C); given their size, the slopes imply a poorer relationship between detected cases and WWTP daily viral RNA load, and intercepts a poorer sensitivity than expected. These WWTPs are defined by fragmented and highly dispersed CAs compared to most WWTPs of this size. Thus network architecture may be important, and sub-catchment sampling may be necessary for large, fragmented, and/or dispersed networks. Deprivation also had a significant impact on the intercept, possibly due to differences in case reporting and/or viral RNA load per case, or the impact of higher industrial discharge. Combined, these factors meant that the limit of detection of cases per 100,000 population was highly variable between WWTPs: median[interquartile] 9·2 [5·6-16·9] for the smaller sites, 19·8 [9·4-31·9] for the medium-sized sites, and 10·8 [6·2-24·6] for the larger sites.

In contrast to most previous studies <sup>21,25-27,30</sup>, we demonstrate the value of obtaining flow measurements from WWTPs to calculate daily viral RNA loads, which display a stronger correlation with detected community case numbers, compared with viral concentration data alone (Fig S2.7). The daily influent flow is mostly affected by the weather and the WWTP size and, because of the latter, the correlation between flow and population connected to the WWTP sewage system is very strong (see Fig S2.6). The improvement of the correlations and model performance observed when using the daily viral load suggest that, not only can this substitute for scaling the cases by the total population, but that it might include other effects (i.e. dilution or weather) which would remain hidden otherwise. Our Spearman's rank correlation  $\rho = 0.79$  when not normalizing using the influent flow rate

388 is almost identical to  $\rho = 0.73$  reported by other authors<sup>23</sup>, who obtained mixed results  
389 when attempting to normalize using other methods, and serves to further highlight the  
390 utility of normalizing using influent flow rate.

391 Our typically low limits of detection show that wastewater surveillance can be particularly  
392 valuable for areas reaching low prevalence and is therefore suitable as a logistically  
393 sustainable early warning system, making a targeted community testing strategy viable. For  
394 WWTPs collecting wastewater from cities, it is harder to isolate small clusters of infections.  
395 This hurdle can be overcome by sampling a site “upstream” to the WWTP (i.e. within the  
396 sewerage network) to improve spatial resolution. This is currently taking place in Scotland,  
397 with local health boards using sub-catchment wastewater sampling to direct surge testing.  
398 For smaller catchments, the size and the spatial resolution is already fine enough to inform  
399 community interventions, however a potential issue here is the variability in the signal.  
400 Specifically, we observed sudden spikes in the viral RNA load or viral concentration in many  
401 small WWTPs (Fig 2, E and F; Fig S2.4; Fig S2.5). While smaller catchments might be more  
402 sensitive to individual variations in shedding, these spikes might also be caused by one or  
403 two households being infected in a short period of time. Given the sensitivity of these  
404 smaller WWTPs to a small number of cases, this may explain these sudden variations in the  
405 SARS-CoV-2 daily viral RNA load. This also raises important questions with respect to the  
406 frequency of sampling, where it may be necessary to sample smaller sites more frequently  
407 to ensure that brief intense signals are not missed.

408 Whilst we have shown that daily viral RNA load has the best correlation with detected cases  
409 (Figure S2.7), daily WWTP flow measurements are not always available. This may be more of  
410 a problem in smaller WWTPs, where flow rates regularly exceed the working range of the  
411 flow meter or in low resource settings, however our model retained substantial detection



power when daily flow was estimated using easily obtained ammonium concentrations, with the conditional  $R^2$  dropping by only 2% ( $R^2 = 0.76$ ).

To better understand the relationship between WWTP viral RNA load and infected individuals, we need to consider the level of viral shedding in feces and how this varies over time. Whilst SARS-CoV-2 RNA can be detected in the feces of hospitalized patients for over four weeks <sup>28, 29</sup>, our work and that of others <sup>30</sup> implies a relatively short period of time over which infected individuals substantially contribute to the wastewater signal. This was observed in two distinct sensitivity analyses, one on correlations and the other on mixed model performance (see Supporting Information). Specifically, the correlation between cases and viral RNA load (and between positive test rate and viral concentration) stabilizes once detected cases are included up to and including the five days prior to wastewater sampling. Furthermore, even with declining incidence, when the cumulative effect of older infections would be expected to have a greater contribution to the overall signal if shedding duration was long, the conditional  $R^2$  of the mixed models did not deteriorate significantly (0.76 compared to 0.78 when incidence was increasing), and was consistent with a short period of peak viral shedding. Unfortunately, there is currently very limited data on fecal shedding of SARS-CoV-2 RNA in non-hospitalized individuals. Our understanding of the relationship between the WWTP viral RNA load and infected individuals is further complicated by the biases in community testing and movement (although restricted during lockdowns) of individuals between CAs. Specifically, testing of symptomatic individuals is unlikely to fully reflect the population incidence, with an analysis of English data suggesting that approximately 1 in 4 cases were being reported via community testing up to November 2020 <sup>31</sup>. It is therefore likely that the model in this study underestimates the true prevalence of infection within the community. It is also possible that factors that have not been

considered in this study, such as the degree of movement in and out of a CA, complicate the relationship between WWTP viral load and reported cases attributed to residents within the CA.

The value of our results extends beyond the first year of the COVID-19 pandemic. We have demonstrated how COVID-19 WBE can be implemented at a national scale across a diverse range of urban and remote communities. At the time of writing, this program has been expanded to cover 75% of the population of Scotland and is being used by local health boards to direct surge testing within the community. This program will continue to be important during the rollout of COVID-19 vaccinations, particularly with respect to disclosing areas of on-going disease transmission and surveillance for novel SARS-CoV-2 variants <sup>32, 33</sup>.

There is currently no data comparing the fecal shedding of SARS-CoV-2 RNA between different variants, however the lower Ct values observed in respiratory swabs from patients infected with variant B.1.617.2 (Delta) <sup>34</sup> imply that fecal shedding may also vary between some variants. It is possible that models that relate influent viral load to cases within the community may need to be adjusted in the future to account for the prevalence of specific variants within the population served by the WWTP CA. It also provides public health authorities with an unbiased surveillance network for other viral and bacterial infections, including antimicrobial resistance genes, shed in feces. Until the COVID-19 pandemic, WBE was predominantly limited to the surveillance of a narrow range of viruses (e.g. polio, norovirus, Hepatitis A/E) in low resource, sewerage settings <sup>35-37</sup>. This study demonstrates the rapid inception, development, validation and operationalization of a national COVID-19 WBE program to provide community surveillance during the pandemic.

459    **Supporting information:** Additional experimental details, materials, methods and results,  
460    including the relationships between SARS-CoV-2 viral RNA concentration or load and test  
461    positivity or reported cases for each wastewater treatment plant included in the study.

462

463

## Acknowledgements

This study was funded by project grants from the Scottish Government via the Centre of Expertise for Waters (CD2019/06) and The Natural Environment Research Council's COVID-19 Rapid Response grants (NE/V010441/1). The Roslin Institute receives strategic funding from the Biotechnology and Biological Sciences Research Council (BB/P013740/1, BBS/E/D/20002173). Sample collection and supplementary analysis was funded and undertaken by Scottish Water and the majority of the sample analysis was funded and undertaken by the Scottish Environment Protection Agency.

The authors would like to thank all the sampling and courier staff at Scottish Water and the team of scientists and other staff at the Scottish Environment Protection Agency for their efforts in acquiring, transporting and analyzing the wastewater samples throughout the pandemic, as well as the electronic Data Research and Innovation Service (eDRIS) who provided the COVID-19 test and death data. We would also like to acknowledge the support of Andrew Millar, the Scottish Government's Chief Scientific Adviser for Environment, Natural Resources and Agriculture.

## References

1. Aguiar-Oliveira, M. L.; Campos, A.; A, R. M.; Rigotto, C.; Sotero-Martins, A.; Teixeira, P. F. P.; Siqueira, M. M., Wastewater-Based Epidemiology (WBE) and Viral Detection in Polluted Surface Water: A Valuable Tool for COVID-19 Surveillance-A Brief Review. *Int J Environ Res Public Health* **2020**, *17*, (24).
2. Polo, D.; Quintela-Baluja, M.; Corbishley, A.; Jones, D. L.; Singer, A. C.; Graham, D. W.; Romalde, J. L., Making waves: Wastewater-based epidemiology for COVID-19 - approaches and challenges for surveillance and prediction. *Water Res* **2020**, *186*, 116404.
3. Medema, G.; Been, F.; Heijnen, L.; Pettersen, S., Implementation of environmental surveillance for SARS-CoV-2 virus to support public health decisions: Opportunities and challenges. *Curr Opin Environ Sci Health* **2020**, *17*, 49-71.
4. Kitajima, M.; Ahmed, W.; Bibby, K.; Carducci, A.; Gerba, C. P.; Hamilton, K. A.; Haramoto, E.; Rose, J. B., SARS-CoV-2 in wastewater: State of the knowledge and research needs. *Science of The Total Environment* **2020**, 139076.
5. Hoffmann, T.; Alsing, J., Faecal shedding models for SARS-CoV-2 RNA amongst hospitalised patients and implications for wastewater-based epidemiology. *medRxiv* **2021**, 2021.03.16.21253603.
6. Medema, G.; Heijnen, L.; Elsinga, G.; Italiaander, R.; Brouwer, A., Presence of SARS-Coronavirus-2 RNA in Sewage and Correlation with Reported COVID-19 Prevalence in the Early Stage of the Epidemic in The Netherlands. *Environmental Science & Technology Letters* **2020**, *7*, (7), 511-516.
7. Naughton, C. C.; Roman, F. A.; Alvarado, A. G. F.; Tariqi, A. Q.; Deeming, M. A.; Bibby, K.; Bivins, A.; Rose, J. B.; Medema, G.; Ahmed, W.; Katsivelis, P.; Allan, V.; Sinclair, R.; Zhang, Y.; Kinyua, M. N., Show us the Data: Global COVID-19 Wastewater Monitoring Efforts, Equity, and Gaps. *medRxiv* **2021**, 2021.03.14.21253564.
8. European Commission, HERA Incubator: Anticipating together the threat of COVID-19 variants. In Brussels, 2021.
9. Scottish Environment Protection Agency (SEPA) RNAMonitoring. <https://informatics.sepa.org.uk/RNAMonitoring/>
10. National Records of Scotland Population Estimates by Scottish Index of Multiple Deprivation (SIMD). <https://www.nrscotland.gov.uk/statistics-and-data/statistics/statistics-by-theme/population/population-estimates/2011-based-special-area-population-estimates/population-estimates-by-simd-2016>
11. Dohoo, I. R.; Martin, S. W.; Stryhn, H., *Methods in Epidemiologic Research*. VER Incorporated: 2012.
12. Johnson, P. C. D., Extension of Nakagawa & Schielzeth's R<sup>2</sup>GLMM to random slopes models. *Methods in Ecology and Evolution* **2014**, *5*, (9), 944-946.
13. Team, R. C., R: A language and environment for statistical computing. **2020**.
14. Wickham, H.; Averick, M.; Bryan, J.; Chang, W.; McGowan, L.; François, R.; Golemund, G.; Hayes, A.; Henry, L.; Hester, J.; Kuhn, M.; Pedersen, T.; Miller, E.; Bache, S.; Müller, K.; Ooms, J.; Robinson, D.; Seidel, D.; Spinu, V.; Takahashi, K.; Vaughan, D.; Wilke, C.; Woo, K.; Yutani, H., Welcome to the Tidyverse. *Journal of Open Source Software* **2019**, *4*, (43), 1686.
15. Wickham, H.; Seidel, D., scales: Scale Functions for Visualization. **2020**.
16. Slowikowski, K., ggrepel: Automatically Position Non-Overlapping Text Labels with 'ggplot2'. **2021**.

17. Bates, D.; Mächler, M.; Bolker, B.; Walker, S., Fitting Linear Mixed-Effects Models Using lme4. *2015* **2015**, 67, (1), 48.
18. Barton, K., MuMIn: Multi-Model Inference. . **2020**.
19. Graham, K. E.; Loeb, S. K.; Wolfe, M. K.; Catoe, D.; Sinnott-Armstrong, N.; Kim, S.; Yamahara, K. M.; Sassoubre, L. M.; Mendoza Grijalva, L. M.; Roldan-Hernandez, L.; Langenfeld, K.; Wigginton, K. R.; Boehm, A. B., SARS-CoV-2 RNA in Wastewater Settled Solids Is Associated with COVID-19 Cases in a Large Urban Sewershed. *Environmental Science & Technology* **2021**, 55, (1), 488-498.
20. Wang, X., fANCOVA: Nonparametric Analysis of Covariance. **2020**.
21. Peccia, J.; Zulli, A.; Brackney, D. E.; Grubaugh, N. D.; Kaplan, E. H.; Casanovas-Massana, A.; Ko, A. I.; Malik, A. A.; Wang, D.; Wang, M.; Warren, J. L.; Weinberger, D. M.; Arnold, W.; Omer, S. B., Measurement of SARS-CoV-2 RNA in wastewater tracks community infection dynamics. *Nature Biotechnology* **2020**, 38, (10), 1164-1167.
22. Wolfe, M. K.; Archana, A.; Catoe, D.; Coffman, M. M.; Dorevich, S.; Graham, K. E.; Kim, S.; Grijalva, L. M.; Roldan-Hernandez, L.; Silverman, A. I.; Sinnott-Armstrong, N.; Vugia, D. J.; Yu, A. T.; Zambrana, W.; Wigginton, K. R.; Boehm, A. B., Scaling of SARS-CoV-2 RNA in Settled Solids from Multiple Wastewater Treatment Plants to Compare Incidence Rates of Laboratory-Confirmed COVID-19 in Their Sewersheds. *Environmental Science & Technology Letters* **2021**, acs.estlett.1c00184.
23. Feng, S.; Roguet, A.; McClary-Gutierrez, J. S.; Newton, R. J.; Kloczko, N.; Meiman, J. G.; McLellan, S. L., Evaluation of Sampling, Analysis, and Normalization Methods for SARS-CoV-2 Concentrations in Wastewater to Assess COVID-19 Burdens in Wisconsin Communities. *ACS ES&T Water* **2021**, 1, (8), 1955-1965.
24. Wu, F.; Xiao, A.; Zhang, J.; Moniz, K.; Endo, N.; Armas, F.; Bushman, M.; Chai, P. R.; Duvallet, C.; Erickson, T. B.; Foppe, K.; Ghaeli, N.; Gu, X.; Hanage, W. P.; Huang, K. H.; Lee, W. L.; McElroy, K. A.; Rhode, S. F.; Matus, M.; Wuertz, S.; Thompson, J.; Alm, E. J., Wastewater surveillance of SARS-CoV-2 across 40 U.S. states from February to June 2020. *Water research* **2021**, 202, 117400-117400.
25. Ahmed, W.; Angel, N.; Edson, J.; Bibby, K.; Bivins, A.; O'Brien, J. W.; Choi, P. M.; Kitajima, M.; Simpson, S. L.; Li, J.; Tschärke, B.; Verhagen, R.; Smith, W. J. M.; Zaugg, J.; Dierens, L.; Hugenholtz, P.; Thomas, K. V.; Mueller, J. F., First confirmed detection of SARS-CoV-2 in untreated wastewater in Australia: A proof of concept for the wastewater surveillance of COVID-19 in the community. *Science of The Total Environment* **2020**, 138764.
26. Wurtzer, S.; Marechal, V.; Mouchel, J.; Maday, Y.; Teyssou, R.; Richard, E.; Almayrac, J.; Moulin, L., Evaluation of lockdown effect on SARS-CoV-2 dynamics through viral genome quantification in waste water, Greater Paris, France, 5 March to 23 April 2020. *Eurosurveillance* **2020**, 25, (50), 2000776.
27. Randazzo, W.; Truchado, P.; Cuevas-Ferrando, E.; Simn, P.; Allende, A.; Snchez, G., SARS-CoV-2 RNA in wastewater anticipated COVID-19 occurrence in a low prevalence area. *Water Research* **2020**, 115942.
28. Xu, Y.; Li, X.; Zhu, B.; Liang, H.; Fang, C.; Gong, Y.; Guo, Q.; Sun, X.; Zhao, D.; Shen, J.; Zhang, H.; Liu, H.; Xia, H.; Tang, J.; Zhang, K.; Gong, S., Characteristics of pediatric SARS-CoV-2 infection and potential evidence for persistent fecal viral shedding. *Nature Medicine* **2020**, 1--4.
29. Xing, Y. H.; Ni, W.; Wu, Q.; Li, W. J.; Li, G. J.; Wang, W. D.; Tong, J. N.; Song, X. F.; Wing-Kin Wong, G.; Xing, Q. S., Prolonged viral shedding in feces of pediatric patients with coronavirus disease 2019. *J Microbiol Immunol Infect* **2020**, 53, (3), 473-480.

30. Wu, F.; Xiao, A.; Zhang, J.; Gu, X.; Lee, W. L.; Kauffman, K.; Hanage, W.; Matus, M.; Ghaeli, N.; Endo, N.; Duvallet, C.; Moniz, K.; Erickson, T.; Chai, P.; Thompson, J.; Alm, E., SARS-CoV-2 titers in wastewater are higher than expected from clinically confirmed cases. *medRxiv* **2020**, 2020.04.05.20051540.
31. Colman, E.; Enright, J.; Puspitarani, G. A.; Kao, R. R., Estimating the proportion of SARS-CoV-2 infections reported through diagnostic testing. *medRxiv* **2021**, 2021.02.09.21251411.
32. Crits-Christoph, A.; Kantor, R. S.; Olm, M. R.; Whitney, O. N.; Al-Shayeb, B.; Lou, Y. C.; Flamholz, A.; Kennedy, L. C.; Greenwald, H.; Hinkle, A.; Hetzel, J.; Spitzer, S.; Koble, J.; Tan, A.; Hyde, F.; Schroth, G.; Kuersten, S.; Banfield, J. F.; Nelson, K. L., Genome Sequencing of Sewage Detects Regionally Prevalent SARS-CoV-2 Variants. *mBio* **2021**, *12*, (1).
33. Covid-Genomics UK consortium, An integrated national scale SARS-CoV-2 genomic surveillance network. *Lancet Microbe* **2020**, *1*, (3), e99-e100.
34. Williams, G. H.; Llewelyn, A.; Brandao, R.; Chowdhary, K.; Hardisty, K.-M.; Loddo, M., SARS-CoV-2 testing and sequencing for international arrivals reveals significant cross border transmission of high risk variants into the United Kingdom. *EClinicalMedicine* **2021**, *38*, 101021-101021.
35. Deshpande, J. M.; Shetty, S. J.; Siddiqui, Z. A., Environmental surveillance system to track wild poliovirus transmission. *Appl Environ Microbiol* **2003**, *69*, (5), 2919-27.
36. Farkas, K.; Cooper, D. M.; McDonald, J. E.; Malham, S. K.; de Rougemont, A.; Jones, D. L., Seasonal and spatial dynamics of enteric viruses in wastewater and in riverine and estuarine receiving waters. *Sci Total Environ* **2018**, *634*, 1174-1183.
37. Miura, T.; Lhomme, S.; Le Saux, J. C.; Le Mehaute, P.; Guillois, Y.; Couturier, E.; Izopet, J.; Abranavel, F.; Le Guyader, F. S., Detection of Hepatitis E Virus in Sewage After an Outbreak on a French Island. *Food Environ Virol* **2016**, *8*, (3), 194-9.